**Chemistry–A European Journal**

Research Article
doi.org/10.1002/chem.202203963

Chemistry
Europe
European Chemical
Societies Publishing

Check for updates

www.chemeurj.org

# Across the Dimensions: A Three-Component Self-Assembly of Pentaphosphaferrocene-based Coordination Polymers

Kevin Grill,[a] Sabrina B. Dinauer,[a] Eugenia Peresypkina,[a] Alexander V. Virovets,[b] and Manfred Scheer*[a]

**Abstract:** Pentaphosphaferrocenes $[Cp^RFe(\eta^5\text{-}P_5)]$ ($Cp^* = \eta^5\text{-}C_5Me_5$) (**A**), $Cp'' = \eta^5\text{-}C_5H_3tBu_2\text{-}1,3$ (**B**)) are excellent building blocks for polymeric assemblies in supramolecular chemistry in combination with coinage metal salts of weakly coordinating anions such as $AgSbF_6$. Adding rigid aromatic dinitriles *ortho/meta/para*-$(NC)_2C_6H_4$ in a one-pot reaction between $[Cp^RFe(\eta^5\text{-}P_5)]$ and $AgSbF_6$ leads to various coordination polymers (CPs) by a three-component self-assembly. The sterical demand of the differently substituted cyclopentadiene ligands as well as the rigid constitution of the isomeric dinitriles $(NC)_2C_6H_4$ play a key role in the formation of the isolated CPs. All CPs were characterized by NMR spectroscopy, mass spectrometry, elemental analysis, and single-crystal X-ray diffraction.

## Introduction

Based on the interdisciplinary impact of chemistry, physics and biology on supramolecular chemistry, this area presents one of the most fascinating and rapidly growing topics in current chemistry. Due to both versatility and variability, supramolecular chemistry spans a broad field of research and applications for example in drug delivery, catalysis, molecular storage, etc..[1] Supramolecular chemistry relies on the concept of molecular self-assembly[2] and focuses mostly rather weak interactions such as hydrogen bonding, van der Waals or π–π interactions.[3] Some supramolecular assemblies are large enough to create cavities for smaller guest molecules.[4] Additionally, metallosupramolecular chemistry uses metal ions as fundamental building blocks beside organic ligands.[5] Hence, well-defined reaction conditions as well as a sophisticated molecular design of the used building blocks are required.[6]

First studies in this challenging field of metallosupramolecular chemistry were highlighted by Fujita and Ogura in 1990 with the self-assembly of Pd(II)-based macrocyclic[7] and polymeric structures. Beside the first tetranuclear square complex $[(en)Pd(4,4'\text{-}bpy)]_4(NO_3)_8$, which attracted considerable interest,[8] the authors were also able to obtain a 2D coordination network consisting of Cd(II) and 4,4'−bipyridine.[9] Imparting this system more flexibility by using benzene-based ligands with flexible pyridine arms, resulted in the formation of infinite networks of ladders and bricks.[10] These infinite polycatenane frameworks consist of 60-membered rings (ladder) or 90-membered rings (brick) and show the influence of the organic ligands on the resulting connectivity of the supramolecular assembly. Therefore, the choice of the organic ligand has, on the one hand, a decisive impact on the freedom of the self-assembly system and, on the other hand, the system can be controlled via modifications of the ligand.[11]

Moreover, the metal center and therefore the associated metal salt has a considerable impact on the system as well. Among coinage metals, gold being a two-coordinate cation has a linear or planar coordination geometry around the metal center,[12] scarcely providing sufficient coordination sites. Copper(I) cations supply from three to four coordination sites, however, copper salts either contain copper complex cations with coordinated solvent molecules or dissolve in organic media only upon complexation with solvents as for instance acetonitrile, which would compete with the targeted organic ligand for coordination and uncontrollably block coordination sites at the metal center. To grant free coordination sites at the metal centers, one is restricted to using non-blocking counterions or solvents. However, the silver salt of the non-coordinating anion $SbF_6^-$ lacks the aforesaid disadvantages and is known, together with polyphosphorus ligands, to build supramolecular assemblies bearing free coordination sites at the silver centers that can be immediately coordinated by N-donor ligands in a one-step self-assembly reaction.[13]

As we have already shown, that the polyphosphorus complexes used in two-component self-assembly reactions with $[Cp^RFe(\eta^5\text{-}P_5)]$ ($Cp^R = Cp^*$ (**A**), $Cp^{Bn} = Cp(CH_2Ph)_5$) and CuX (X = Cl, Br, I or triflate) or $CuX_2$ (X = Cl, Br) form various spherical aggregates with host-guest properties.[14] Their reactivity relies on the substituent-free P atoms that are solely bound to other

[a] K. Grill, S. B. Dinauer, Dr. E. Peresypkina, Prof. Dr. M. Scheer
Institute of Inorganic Chemistry
University of Regensburg
Universitätsstraße 31, 93040 Regensburg (Germany)
E-mail: Manfred.Scheer@ur.de

[b] Dr. A. V. Virovets
Institute of Inorganic Chemistry
Goethe-University Frankfurt am Main
Max-von-Laue-Straße 7, 60438 Frankfurt am Main (Germany)

P or metal atoms which influence the steric and electronic properties of the coordinating P atoms and therefore enable a unique coordination chemistry.

Combining polyphosphorus complexes with $AgSbF_6$ and organic ligands lead to a three-component self-assembly system possessing flexibility, variability, and versatility, therefore showing a high potential for the formation of both supramolecular assemblies and multi-dimensional coordination polymers.

Following this idea, with the aim to obtain such supramolecular aggregates, we have recently reported a controllable one-pot three-component self-assembly system consisting of **A**, $AgSbF_6$ and flexible aliphatic dinitriles of the type $NC(CH_2)_xCN$ ($x = 1$–10).[15] Surprisingly, we observed that the length and flexibility of an aliphatic chain of the organic ligand influence the outcome of the self-assembly system. By increasing the length of the aliphatic dinitrile and therefore giving the system more and more adjusting capabilities, the system builds different 1D–3D coordination polymers with short linkers ($x \leq 6$), and astonishingly changes its course in the case of longer linkers ($x \geq 7$) where it leads to nanosized organometallic host-guest spherical assemblies connected in various 3D supramolecular coordination networks.

This fact raises the question as to what will happen if the three-component self-assembly system is restricted to some extent. On the one hand, more sterically demanding polyphosphorus complexes can be used, which should strongly influence the coordination sphere of a metal cation due to the increasing steric hinderance. Additionally, the solubility of the polyphosphorus complex will change, which would also influence the respective reaction conditions.[16] On the other hand, choosing
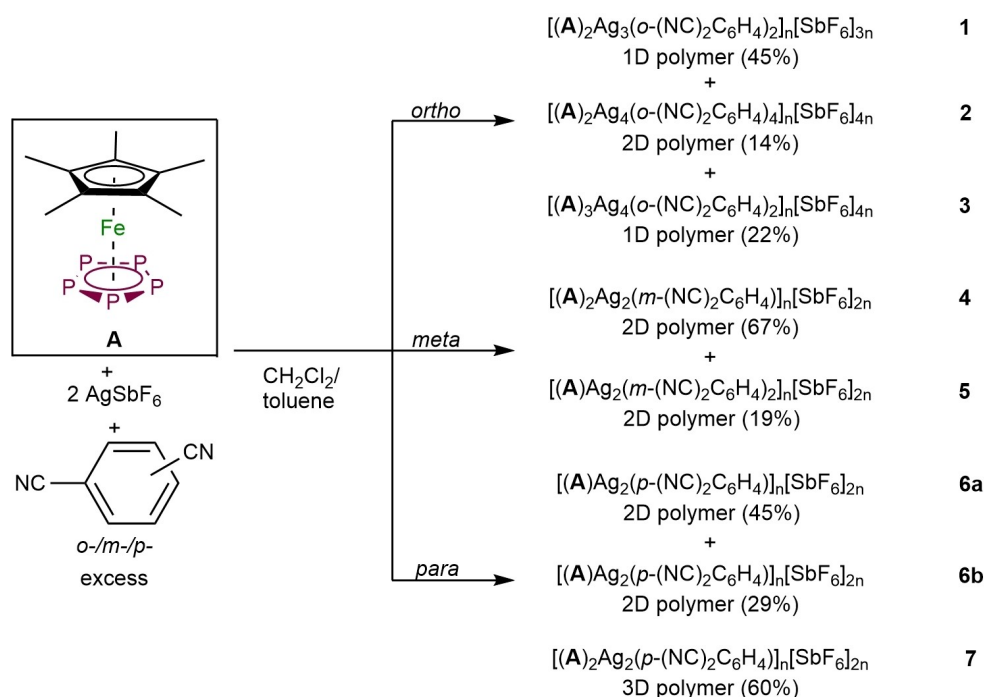
more rigid organic linkers with fixed bite angles and a known arrangement of the donor groups could lead to a more controllable outcome.

With these considerations in mind, we decided to use the isomers of the rigid aromatic dinitrile ortho/meta/para-$(NC)_2C_6H_4$ as organic linker, due to the electronic effects of the aromatic part and the fixed angles, and, besides **A**, another polyphosphorus complex with a slightly higher sterical demand $[Cp''Fe(\eta^5-P_5)]$ ($Cp'' = \eta^5-C_5H_3tBu_2$-1,3 (**B**)) to study the influence of sterical hinderance of two tBu groups onto the self-assembly outcome. Herein we report a systematic study of the three-component self-assembly system of **A** or **B** polyphosphorus building blocks, $AgSbF_6$ and rigid aromatic dinitriles ortho/meta/para-$(NC)_2C_6H_4$ showing that the resulting coordination polymers of different dimensionalities and connectivity are accessible depending on the position of the nitrile functionalities in the dinitrile ligands and the sterical influence of the cyclopentadienyl ligand of the substituted pentaphosphaferrocene. The influence of these factors on the products of the self-assembly is analysed.

## Results and Discussion

### Three-component self-assembly using $[Cp*Fe(\eta^5-P_5)]$ (A)

For all reactions, a solution of $AgSbF_6$ in $CH_2Cl_2$ was first layered with a mixture of $CH_2Cl_2$ and toluene (2:1) and then with a toluene solution of **A** and the isomeric rigid aromatic dinitrile $o/m/p$-$(NC)_2C_6H_4$. The one-pot reactions were controlled via using different concentrations in the respective layers and a ratio of **A**:2 Ag (Scheme 1). The corresponding dinitrile was added in a



$[(\mathbf{A})_2Ag_3(o\text{-}(NC)_2C_6H_4)_2]_n[SbF_6]_{3n}$ **1**
1D polymer (45%)
+
$[(\mathbf{A})_2Ag_4(o\text{-}(NC)_2C_6H_4)_4]_n[SbF_6]_{4n}$ **2**
2D polymer (14%)
+
$[(\mathbf{A})_3Ag_4(o\text{-}(NC)_2C_6H_4)_2]_n[SbF_6]_{4n}$ **3**
1D polymer (22%)

$[(\mathbf{A})_2Ag_2(m\text{-}(NC)_2C_6H_4)]_n[SbF_6]_{2n}$ **4**
2D polymer (67%)
+
$[(\mathbf{A})Ag_2(m\text{-}(NC)_2C_6H_4)_2]_n[SbF_6]_{2n}$ **5**
2D polymer (19%)

$[(\mathbf{A})Ag_2(p\text{-}(NC)_2C_6H_4)]_n[SbF_6]_{2n}$ **6a**
2D polymer (45%)
+
$[(\mathbf{A})Ag_2(p\text{-}(NC)_2C_6H_4)]_n[SbF_6]_{2n}$ **6b**
2D polymer (29%)

$[(\mathbf{A})_2Ag_2(p\text{-}(NC)_2C_6H_4)]_n[SbF_6]_{2n}$ **7**
3D polymer (60%)

**Scheme 1.** One-pot self-assembly reactions of **A**, $AgSbF_6$, and aromatic isomers of $o$-/$m$-/$p$-$(NC)_2C_6H_4$. Isolated crystalline yields are given in parentheses.

Chemistry–A European Journal

Research Article
doi.org/10.1002/chem.202203963

Chemistry
Europe
European Chemical
Societies Publishing

10-fold excess with respect to **A** to prohibit restrictions by the amount of organic ligand in the form of a stock solution or as pure compound. In all reactions, brown laths of the known 1D polymer $[(\mathbf{A})_2Ag]_n[SbF_6]_n$ co-crystallize as byproduct[15] as well as unavoidable colorless crystals of a compound containing $AgSbF_6$ and the respective dinitrile linker. The latter was not of interest due to missing **A** and was not further investigated (see Supporting Information for detail). Noteworthily, a direct synthesis with stoichiometric ratios to the desired products failed despite many attempts, resulting in the mentioned byproducts.

In the reaction of $o\text{-}(NC)_2C_6H_4$, **A** and $AgSbF_6$ with a concentration of 2 mmol L$^{-1}$ in the respective layers, a mixture consisting of a 1D polymer $[\{\mathbf{A}\}_2Ag_3(o\text{-}(NC)_2C_6H_4)_2]_n[SbF_6]_{3n}$ (**1**: brown blocks), a 2D polymer $[\{\mathbf{A}\}_2Ag_4(o\text{-}(NC)_2C_6H_4)_4]_n[SbF_6]_{4n}$ (**2**: yellow plates) and another 1D polymer $[\{\mathbf{A}\}_3Ag_4(o\text{-}(NC)_2C_6H_4)_2]_n$-$[SbF_6]_{4n}$ (**3**: brown laths) were obtained (Scheme 1). All products **1–3** and the co-crystallizing byproducts could be separated manually under the microscope. Changes of the stoichiometric ratio or concentration showed no direct influence on the selectivity of the desired products, but drastically changed the amount of the colorless compound containing only $AgSbF_6$ and the linker. The same reaction conditions in the case of $m\text{-}(NC)_2C_6H_4$ lead to a mixture of two polymeric products, 2D $[\{\mathbf{A}\}_2Ag_2(m\text{-}(NC)_2C_6H_4)]_n[SbF_6]_{2n}$ (**4**: yellow plates) and $[\{\mathbf{A}\}Ag_2(m\text{-}(NC)_2C_6H_4)_2]_n[SbF_6]_{2n}$ (**5**: brown laths) (Scheme 1). Nevertheless, these diluted conditions used in the case of $o/m\text{-}(NC)_2C_6H_4$ could not be successfully applied to the $p\text{-}(NC)_2C_6H_4$ isomer, as no product crystallized in this case. Therefore, the concentration of the respective layers was increased to 4 mmol L$^{-1}$ and a fivefold excess of the corresponding aromatic dinitrile with respect to **A** was used to provide enough organic ligand material and, at the same time, to limit the number of possible byproducts. In this way, two 2D polymeric products were obtained. In the solid state, the two solvatomorphic phases of a compound $[\{\mathbf{A}\}Ag_2(p\text{-}(NC)_2C_6H_4)]_n[SbF_6]_{2n}$ (**6a**: brown blocks and **6b**: yellow needles) were found. Keeping an equimolar ratio of **A**:Ag but increasing the amount of organic linker $p\text{-}(NC)_2C_6H_4$ to a 10-fold excess with respect to **A** leads to a 3D polymer $[\{\mathbf{A}\}_2Ag_2(p\text{-}(NC)_2C_6H_4)]_n[SbF_6]_{2n}$ (**7**: brown prisms) (Scheme 1). Remarkably, when keeping the crystals in mother liquor for at least eight months, the ratio between major and minor products was not observed to change, which makes the possibility of their mutual transformation unlikely.

According to single crystal X-ray structure analysis, the polymers based on **A**, $AgSbF_6$, and the rigid aromatic dinitriles span all dimensionalities from 1D to 3D. All polymers consist of infinite Ag/*cyclo*-P$_5$ 1D subunits (Figures 1–7) decorated by the organic ligands, with the ratio and coordination mode of the *cyclo*-P$_5$ ring to the Ag cations varying, which gives rise to different 1D subunits. In addition, the chemical environment of the isomeric dinitriles seems to predetermine the dimensionality of the formed products to a certain extent. For the *ortho* isomer, 1D and 2D polymers are found, all other isomers lead to the formation of 2D or 3D polymers. This is probably due to the small distance between the nitrile functionalities in $o\text{-}(NC)_2C_6H_4$. Therefore, owing to the smallest bite angle ($\sim 60°$), the *ortho* linker seems to be able to bridge the silver ions in the 1,2-
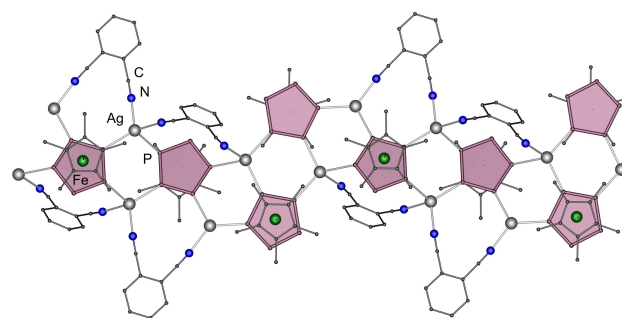


**Figure 1.** The cationic 1D polymer in **1**. H atoms are omitted for clarity.
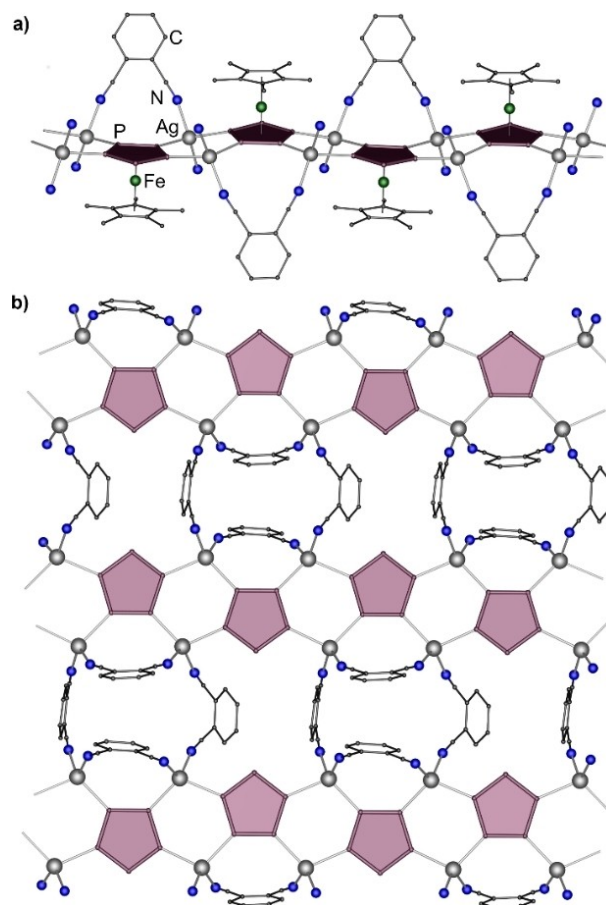


**Figure 2.** The 2D cationic network of **2**: a) a section of the cationic motif $[\{\mathbf{A}\}_2Ag_4]_n^{4n+}$, b) 2D cationic network with interconnecting $o\text{-}(NC)_2C_6H_4$ ligands. H atoms are omitted for clarity.

positions of the *cyclo*-P$_5$ ligands, which leads to 1D chain polymers (Figures 1 and 3), but can also interconnect 1D subunits to give a 2D polymer (Figure 2). With an increasing distance between the nitriles of the linker, 2D (*meta/para*) and 3D polymers (*para*) are more likely to be formed. In the last two cases, the isomeric aromatic rigid linkers act only as a cross-linking spacer to give rise to more extended infinite networks.

The 1D polymer in **1** is built up by $[\{\mathbf{A}\}_2Ag_3]^{3+}$ units, with the *cyclo*-P$_5$ ligands of **A** coordinating to the Ag atoms in
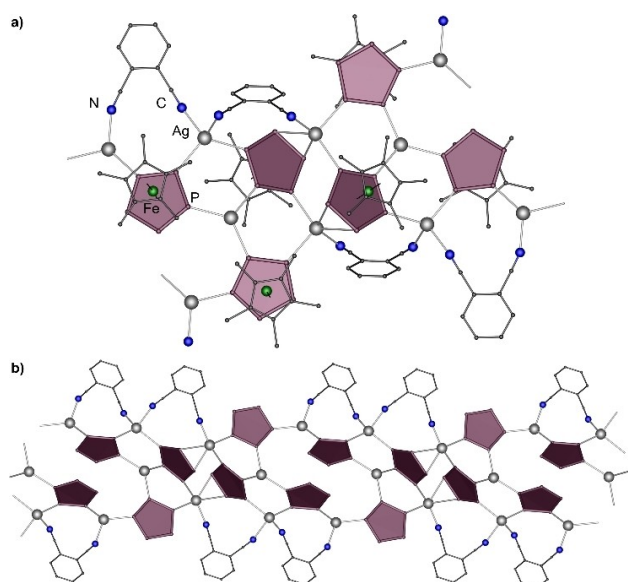
**Figure 3.** Structure of a) the repeating unit and b) a section of the 1D polymer [{**A**}$_3$Ag$_4$(o-(NC)$_2$C$_6$H$_4$)$_2$]$_n^{4n+}$ (**3**). H atoms are omitted for clarity.

alternating 1,2,3- and 1,2,3,4-coordination modes (Figure 1), with Ag ions being tetrahedrally or trigonally coordinated, building the six-membered rings of {P$_4$Ag$_2$} of the 1D chain. The organic ligand coordinates always to a tetrahedrally and a trigonally coordinated Ag atom on the side of the chain. All tetrahedrally coordinated Ag atoms are linked to two organic ligands and two cyclo-P$_5$ ligands, while the Ag atoms in the trigonal environment coordinate to one organic ligand and two cyclo-P$_5$ ligands. The Cp* ligands of **A** alternate in opposite directions with respect to the P$_5$ rings.

The 2D polymer **2** consists of parallel 1D strands [{**A**}$_2$Ag$_4$]$_n^{4n+}$. All cyclo-P$_5$ ligands are coordinated in a 1,2,3,4-mode to Ag atoms (Figure 2). Additionally, two dinitriles are coordinated to each Ag cation completing its tetrahedral environment, while one coordinates to the next silver ion in the same strand and the other binds the silver ion of the next strand. Interestingly, some of the non-bridging dinitriles of each strand face the dinitrile of the next strand, with an interplanar distance of 3.52(1) Å indicating weak π–π interactions due to significantly slipped relative positions of the aromatic systems. Most of the aromatic rings do not participate in stacking as they are isolated by counter anions or solvent molecules of crystallization.

Compared to **1**, the 1D polymer **3** is built up by [{**A**}$_3$Ag$_4$]$_n^{4n+}$ units, with the cyclo-P$_5$ ligands being coordinated in a 1,2,3- or in a 1,2,3,4-coordination mode to the silver cations (Figure 3). Interestingly, the cyclo-P$_5$ ligand coordinates in an η$^{1:2}$-coordination mode to one of the Ag cations, thus forming a pseudo-tetrahedral environment. Therefore, the strands of five six-membered rings and one large 16-membered ring {P$_{12}$Ag$_4$} which separate the adjacent six-membered rings within the strand are built. This distinguishes the structural motif of **3** from that of **1**, which exclusively consists of six-membered rings.

In the reaction of **A**, AgSbF$_6$ and m-(NC)$_2$C$_6$H$_4$, two 2D polymers can be obtained. **4** consists of strands of [{**A**}$_2$Ag$_2$]$_n^{2n+}$, with the cyclo-P$_5$ ligands coordinating in a 1,2,4-coordination mode to Ag atoms (Figure 4a). Additionally, all Ag atoms are coordinated by a dinitrile ligand which completes a tetrahedral environment of the Ag atoms. The dinitriles interconnect two adjacent strands and therefore build the 2D polymeric layer (Figure 4b). The nearest cyclo-P$_5$ ligands in the strand establish a tubular structure with a narrow diameter of 3.41(3) Å, which prevents the encapsulation of solvent molecules or counter ions (Figure 4c).
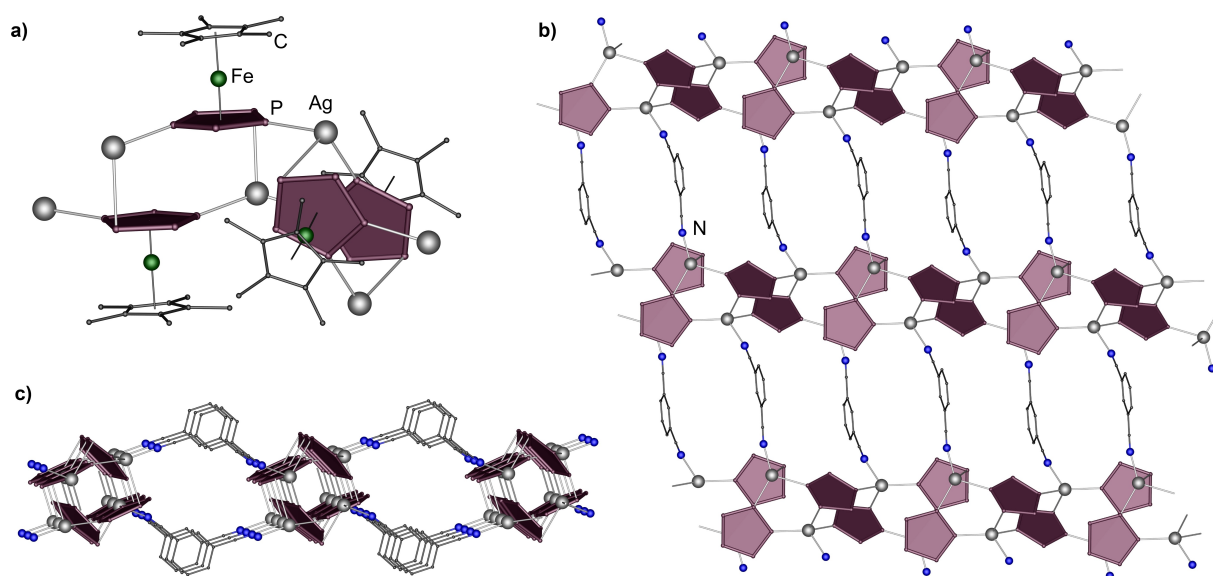


**Figure 4.** The 2D cationic network of **4**. a) tetrameric fragment, b) the strands of **4** are interconnected via bridging m-(NC)$_2$C$_6$H$_4$ ligands, c) tube-like, built up by opposed cyclo-P$_5$ ligands. H atoms are omitted for clarity.

**Chemistry–A European Journal**

Research Article
doi.org/10.1002/chem.202203963

**Chemistry Europe**
European Chemical
Societies Publishing

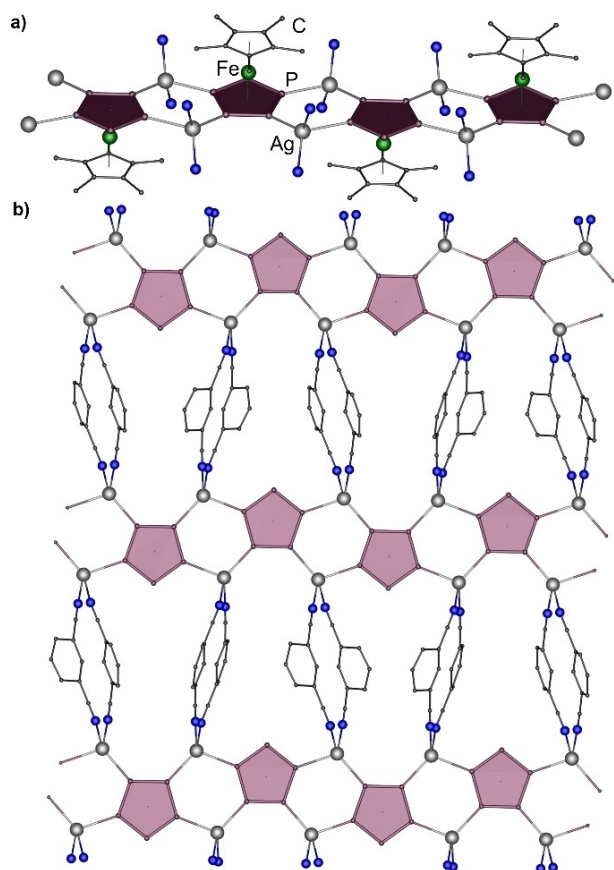**Figure 5.** a) The 1D cationic chain and b) the interconnection through the organic ligand $m\text{-}(NC)_2C_6H_4$ to form the 2D polymer **5**.

The other product of the same reaction but of different stoichiometry gives a new 2D architecture $[\{\mathbf{A}\}Ag_2(p\text{-}(NC)_2C_6H_4)_2]_n^{2n+}$ (**5**), which is also based on similar 1D strands of $[\{\mathbf{A}\}_2Ag_4]_n^{4n+}$ as in **2** and has a similar coordination environment of Ag(I) cations (Figure 5). However, due to the larger bite angle of the ligand, the coordination of the neighbouring Ag ions via bridging dinitrile is prohibited. Instead, in **5**, double dinitrile bridges are formed between a pair of silver atoms belonging to the different chains.

Two 2D polymers of **6a** and **6b** are identical in connectivity and consist of parallel 1D strands $[\{\mathbf{A}\}Ag_2]_n^{2n+}$ units with *cyclo*-$P_5$ ligands coordinating to Ag atoms in a 1,2,3,4-coordination mode, with six-membered rings of $\{P_4Ag_2\}$ being formed (Figure 6). All Ag atoms coordinate to a $p\text{-}(NC)_2C_6H_4$ ligand which leads to trigonally coordinated Ag atoms. The linkers join the 1D strands to a 2D network. Two solvatomorphic modifications are formed in the same crystallization and differ mainly in the solvent portion which, for **6a**, consists of $CH_2Cl_2$ solely and, for **6b**, of toluene and $CH_2Cl_2$. This fact and the relative flexibility of the Ag coordination sphere led to a somewhat different geometrical conformation of the resulting layer (cf. Figure 6b, c). Interestingly, the $\pi$-$\pi$ interactions between the $p\text{-}(NC)_2C_6H_4$ ligands in the smaller meshes of the layers occur in both modifications featuring interplanar distances of 3.22(3) Å for the major position of the disordered ligands (0.55/0.45) and 3.47(2) Å for the minor one (for **6a**), and 3.356(8) Å for **6b**, in which the rigid dinitrile ligands are ordered. The reason for this disorder can arise from the fact that in **6b** the $SbF_6^-$ anion occupies each of the neighboring larger meshes, whereas in **6a** two $CH_2Cl_2$ molecules are disordered in each mesh, that also causes correlated disordering of the ligands. Further difference
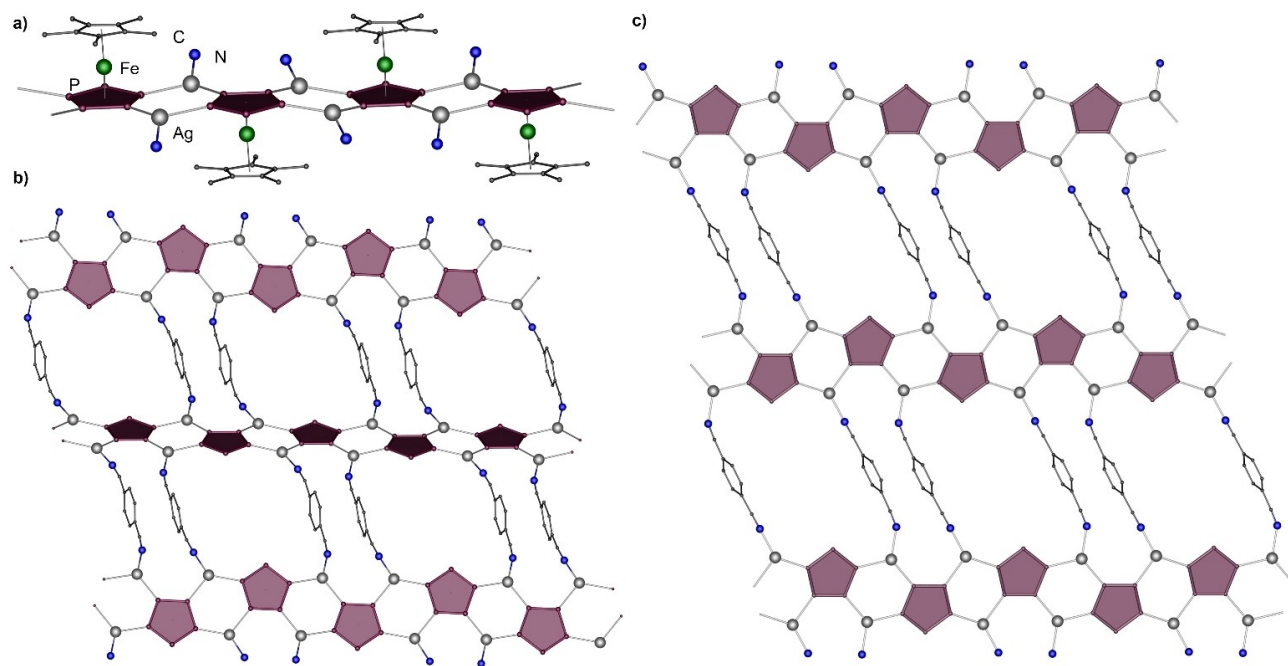


**Figure 6.** A section of the cationic 2D polymers **6a** and **6b**: a) a 1D cationic motif of $[\{\mathbf{A}\}Ag_2]_n^{2n+}$, 1D strands are interconnected by $p\text{-}(NC)_2C_6H_4$ ligands, b) in **6a** and c) in **6b**. H atoms are omitted for clarity.

Chemistry–A European Journal

Research Article
doi.org/10.1002/chem.202203963

**Chemistry Europe**
European Chemical
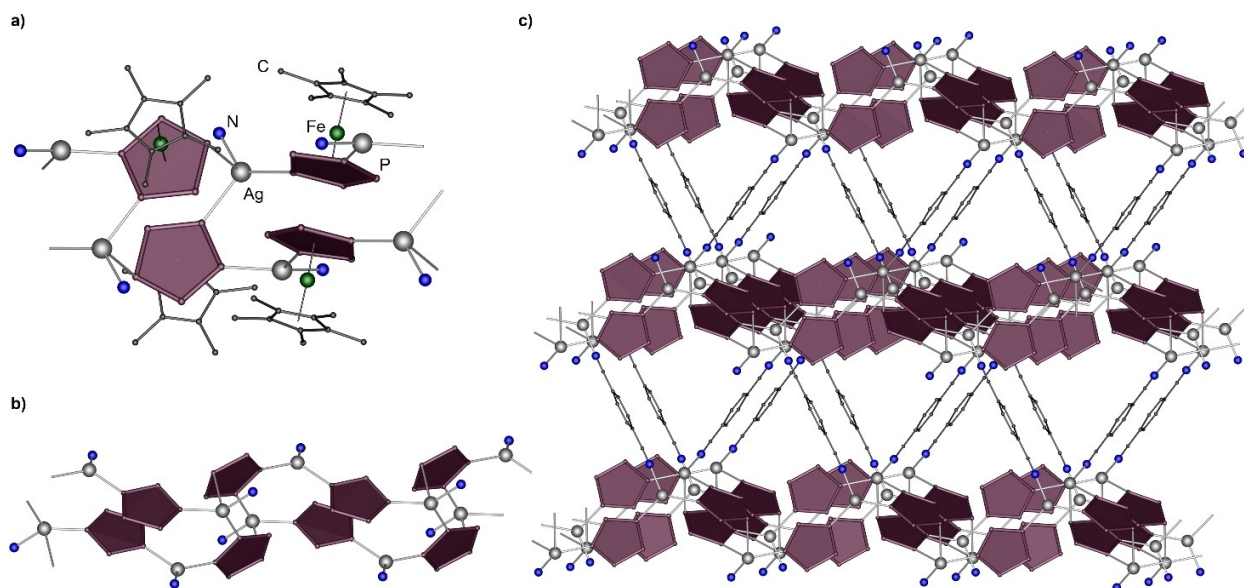Societies Publishing

**Figure 7.** a) Repeating tetrameric unit of a strand in **7**, b) 1D polymeric motif of $[\{A\}_2Ag_2]_n^{2n+}$, c) 3D network in **7**. H atoms are omitted for clarity.

between the solvatomorphs can be found in the space formed by slightly corrugated layers, which is in the case of **6a** occupied by disordered $SbF_6^-$ anions and additional $CH_2Cl_2$ solvent molecules. In **6b**, $SbF_6^-$ anions weakly link and toluene and $CH_2Cl_2$ molecules interlay the 2D sheets. There are no significant Cp*···Cp* interactions found.

Slight adjustments of the reaction conditions led to a 3D polymer **7** with 1D tubular strands of $[\{A\}_2Ag_2]_n^{2n+}$, which are connected via the aromatic linkers (Figure 7). The *cyclo*-$P_5$ ligands coordinate Ag atoms either in a 1,2,4- or in a 1,3-coordination mode. The coordination environment of the Ag cations is completed tetrahedrally or trigonally by $p$-$(NC)_2C_6H_4$ linkers which interconnect the tubular strands to the 3D network. Thus, the linkers are connected to two either tri- or tetra-coordinated Ag cations of the neighbouring 1D strands.
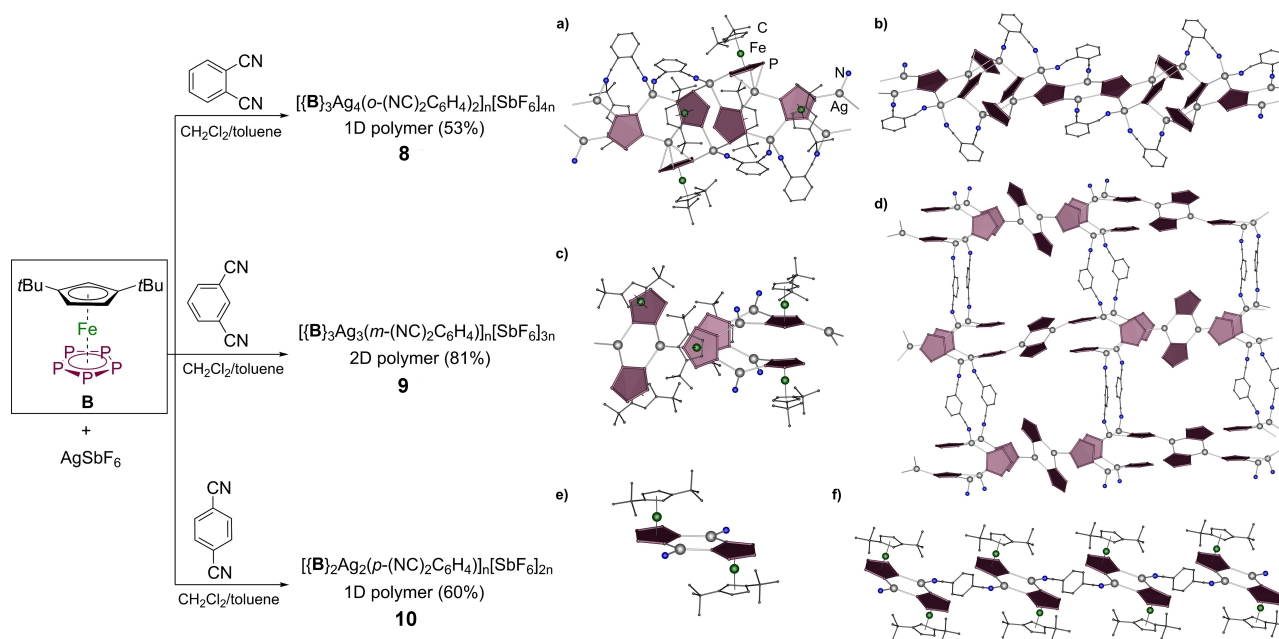
**Three-component self-assembly with [Cp″Fe($\eta^5$-$P_5$)] (B)**

The manifold results of the three-component self-assembly with **A**, $AgSbF_6$ and $o/m/p$-$(NC)_2C_6H_4$ raised the question as to whether the steric bulk of the larger **B** would decidedly influence the self-assembly system. For this purpose, a solution of **B** and a five-fold excess of $o$-$(NC)_2C_6H_4$ with respect to the bulkier **B** in a 1:2 ratio of toluene/hexane (3 mmol L$^{-1}$) was stirred, filtered, and then layered on the mixture of $CH_2Cl_2$ and toluene (2:1) and the already prepared solution of $AgSbF_6$ in $CH_2Cl_2$. This one-pot reaction with the ratio of **B**:2 Ag leads to the 1D coordination polymer of $[\{B\}_3Ag_4(o\text{-}(NC)_2C_6H_4)_2]_n[SbF_6]_{4n}$ (**8**: brown prisms) (Scheme 2). The only possible way to obtain crystals with $m$-$(NC)_2C_6H_4$ was to layer a solution of $AgSbF_6$ in $CH_2Cl_2$ with a mixture of $CH_2Cl_2$ and toluene (2:1) as interlayer and afterwards with a solution of **B** in toluene and a 10-fold excess of the dinitrile with respect to **B** which leads to a 2D

polymer of $[\{B\}_3Ag_3(m\text{-}(NC)_2C_6H_4)]_n[SbF_6]_{3n}$ (**9**: green plates). Under the same reaction conditions, a 1D polymer of $[\{B\}_2Ag_2(p\text{-}(NC)_2C_6H_4)]_n[SbF_6]_{2n}$ (**10**: green plates) is obtained in the reaction with $p$-$(NC)_2C_6H_4$ (Scheme 2). In all reactions, colorless crystals of a compound containing only $AgSbF_6$ and the respective dinitrile co-crystallize as a byproduct and can be separated manually.

The 1D polymeric structure of **8** is severely disordered (see Supporting Information for details); the major part consists of $[\{B\}_3Ag_4]_n^{4n+}$ with the *cyclo*-$P_5$ ligands coordinating to Ag atoms in 1,2,3- or 1,2,3,4-coordination modes (Scheme 2a, b). The dinitrile ligands bridge Ag atoms of the strands. There are four different types of Ag atoms in the crystal structure, one is trigonally coordinated to one linker and two *cyclo*-$P_5$ ligands. The other three are tetrahedrally coordinated; one silver cation coordinates to two different linker molecules and two *cyclo*-$P_5$ ligands, another to one linker and three *cyclo*-$P_5$ ligands, whereas one more $Ag^+$ binds two *cyclo*-$P_5$ ligands in a σ-mode and is $\eta^{1:1:3}$-coordinated to one more *cyclo*-$P_5$ ligand.

For the linker $m$-$(NC)_2C_6H_4$, the resulting 2D polymer **9** is built up by 1D strands of repeating units of $[(B)_3Ag_3]_n^{3n+}$. These parallel strands are connected via the rigid aromatic linkers to give a double square net (Scheme 2c, d). Two *cyclo*-$P_5$ ligands coordinate in a 1,2-mode to a trigonally coordinated Ag atom and therefore build a six-membered ring of $\{P_4Ag_2\}$. The remaining four *cyclo*-$P_5$ ligands build pincer-like 12-membered rings of $\{P_8Ag_4\}$ for steric reasons of accommodating bulky Cp″ ligands in a 2D framework (see Supporting Information for detail). Therefore, these seemingly large channels provide in fact only little space within the in-layer cavities for one outer sphere $SbF_6^-$ anion per cavity. The *cyclo*-$P_5$ ligands in the ring are coordinated in a 1,2,3- or 1,2-coordination mode to an Ag atom in a pseudo-tetrahedral environment. There are no specific interactions between the layers that are interlaid by the

**Chemistry–A European Journal**

Research Article
doi.org/10.1002/chem.202203963

**Chemistry**
**Europe**
European Chemical
Societies Publishing

**Scheme 2.** One-pot self-assembly reactions of **B**, AgSbF$_6$, and isomers of aromatic $o$-/$m$-/$p$-(NC)$_2$C$_6$H$_4$. Isolated crystalline yields are given in parentheses. a) hexameric repeating unit in **8**, b) cationic 1D polymeric strand, c) hexameric [(**B**)$_3$Ag$_3$]$_n^{3n+}$ and d) section of the infinite cationic 2D network in **9**, e) [{**B**}$_2$Ag$_2$]$^{2+}$ subunits comprising, f) 1D polymeric structure of **10**. H atoms are omitted for clarity.

disordered counter anions and toluene and CH$_2$Cl$_2$ solvent molecules.

The 1D polymer **10** with the linker $p$-(NC)$_2$C$_6$H$_4$ is built up by dimeric nodes [{**B**}$_2$Ag$_2$]$_n^{2n+}$, with the $cyclo$-P$_5$ ligands coordinating to trigonally coordinated Ag atoms and therefore building six-membered rings {P$_4$Ag$_2$} (Scheme 2e, f). Each Ag atom has a coordinated linker which interconnects the dimeric nodes to the 1D polymer.

According to the X-ray diffraction, the polymeric compounds built-up by **B**, AgSbF$_6$ and the isomers of (NC)$_2$C$_6$H$_4$ have a 1- or 2-dimensionality. These polymers **8**–**10** consist of finite subunits and 1D chains formed by $cyclo$-P$_5$ building blocks and Ag cations. The nodes consisting of the six-membered rings {P$_4$Ag$_2$} are interconnected by linear $para$ linkers that lead to the formation of a 1D polymeric motif in **10** as expected. The 1D strand formed by P$_5$ rings and silver cations comprises a backbone of the 1D polymer **8**, in which the $ortho$-dinitrile ligands block all silver cations at the sides of the chain from further coordination. 1D strands can also act as subunits connected with the $meta$-isomer of an aromatic dinitrile to an infinite 2D polymer **9**.

## Conclusion

The chosen self-assembly system consisting of [Cp*Fe($\eta^5$-P$_5$)] (**A**) or [Cp″Fe($\eta^5$-P$_5$)] (**B**), AgSbF$_6$ and $o$/$m$/$p$-(NC)$_2$C$_6$H$_4$ gives a remarkable insight into the versatility of rigid aromatic dinitriles and the influence of pentaphosphaferrocenes with different steric demands for the obtained coordination products. The required free coordination sites at the Ag cations for the

coordination of an N-donor ligand besides the polyphosphorus organometallic building blocks **A** and **B** are predesigned by utilizing the weakly coordinating anion SbF$_6^-$ of the respective Ag salt. Using the less sterically demanding **A** clearly led to an increased, but less selective number of coordination products (**1**–**7**), whereas the same reactions with the bulkier **B** are more selective (**8**–**10**). In the systems containing **A**, various coordination polymers with different dimensionalities of up to 3D (**7**) can be isolated, while, for **B**, the formation of coordination polymers is limited by the formation of maximally 2D assemblies (**9**). This may be assumed to depend on the bulkiness of the Cp$^R$ ligand as well as on a better solubility of **B**. Besides this, the used dinitrile plays a crucial role in these systems.

A systematic study with these building blocks highlighted the variability of the configurations of the aromatic dinitrile by changing only one component. For $o$-(NC)$_2$C$_6$H$_4$, mostly 1D polymers (**1**, **3** and **8**) were observed, as the dinitrile molecules themselves bridge the Ag cations of the polymeric arrangements and block their further growth. The only realizable 2D polymer (**2**) was obtained using **A**, as, due to the increased steric demand of the Cp$^R$ ligand **B**, a crosslinking between the 1D strands seems to be hampered. Small 0D subunits that are connected via $p$-(NC)$_2$C$_6$H$_4$ to give the 1D polymer **10** are also achievable as well as the extended 3D polymeric network **7** introducing a higher steric demand by using **B** instead of **A**. The structural motifs of **4**, **5** and **9** based on $m$-(NC)$_2$C$_6$H$_4$ are similar and composed of 2D polymers with the dinitriles crosslinking the 1D subunits. Interestingly, the 1D strands formed by different pentaphosphaferrocenes possess of a similar motif with parallel slipped $cyclo$-P$_5$ ligands, but, in the

**Chemistry–A European Journal**

Research Article
doi.org/10.1002/chem.202203963

**Chemistry Europe**
European Chemical
Societies Publishing

case of **B**, the connectivity sequence is interrupted by a parallel directed cyclo-$P_5$ unit and a trigonal (not tetrahedral) coordination sphere of the adjacent Ag site. The used different isomeric aromatic dinitriles with their different angles between the nitrile-groups still give the three-component self-assembly system enough flexibility within the scope of fixed angles to achieve up to multi-dimensional networks.

These results with rigid dinitriles leading to various polymeric products as well as the previously obtained results with aliphatic flexible dinitriles yielding different 1D/2D/3D polymeric networks and supramolecular networks of host-guest able nodes[15] encourage us to use larger and therefore sterically significantly more demanding polyphosphorus complexes as a next step in further restricting the three-component self-assembly system to study factors leading to the formation of host-guest able nodes connected in a supramolecular network.

## Experimental Section

**General**: Solution NMR spectra were recorded on a Bruker Avance 300 or 400 spectrometer. The corresponding ESI-MS spectra were acquired with a ThermoQuest Finnigan MAT TSQ 7000 mass spectrometer. CHN elemental analysis was performed on a Vario EI III apparatus. All reactions were performed under an inert atmosphere of dry nitrogen with standard vacuum, Schlenk, and glovebox techniques. The solvents were purified, dried, and degassed prior to use by standard procedures. [Cp*Fe($\eta^5$-P$_5$)][17] and [Cp″Fe($\eta^5$-P$_5$)][18] were synthesized according to the reported procedures. The commercially available chemicals AgSbF$_6$ (98%), 1,2-dicyanobenzene, 1,3-dicyanobenzene and 1,4-dicyanobenzene were used without further purification. In all reactions with [Cp*Fe($\eta^5$-P$_5$)] and AgSbF$_6$, the co-crystallization of the by-product [{Cp*Fe($\eta^{5:2:1}$-P$_5$)}$_2$Ag]$_n$[SbF$_6$]$_n$[15] was observed. In all reactions, clear colorless crystals of AgSbF$_6$ with a different amount of o/m/p-(NC)$_2$C$_6$H$_4$ co-crystallized as another by-product (see Supporting Information). Due to the proven absence of cyclo-P$_5$ ligands, these by-products were not further investigated as not interesting. All obtained crystalline solid phases were sorted out manually under the microscope by shape, color or on the diffractometer by the measurement of the unit cell constants. All obtained polymers **1–10** are insoluble in common solvents such as hexane, benzene, toluene, CH$_2$Cl$_2$, thf and Et$_2$O. Yet, all compounds readily dissolve in acetonitrile under degradation of the coordination network. Therefore, in the $^1$H, $^{31}$P{$^1$H} NMR and $^{19}$F spectra of the polymers treated with CD$_3$CN, only signals attributed to the free complexes **A** or **B**, AgSbF$_6$ and dinitriles are detectable.

**Synthesis of 1/2/3**: A solution of AgSbF$_6$ (28 mg, 0.08 mmol) in CH$_2$Cl$_2$ (20 mL) is carefully layered first with a solvent mixture of CH$_2$Cl$_2$/toluene (5 mL, 2:1) and then with a green solution of [Cp*Fe($\eta^5$-P$_5$)] (14 mg, 0.04 mmol) and o-(NC)$_2$C$_6$H$_4$ (1 mL, 0.4 M in CH$_2$Cl$_2$) in toluene (20 mL). After a few hours, the phase boundary turns yellow, and, after one day, the formation of brown blocks of **1** at the phase boundary and yellow plates of **2** and brown laths of **3** slightly below the phase boundary is observed. After complete diffusion, the colorless mother liquor is decanted, the crystals are washed with hexane (3×10 mL) and dried in vacuo. The crystals of **1**, **2** and **3** were separated manually.

**Analytical data of 1/2/3**: **1)** Yield: 36 mg (45% referred to **A**). $^1$H NMR (CD$_3$CN): δ [ppm] = 1.45 (s, [Cp*Fe($\eta^5$-P$_5$)]), 7.82 (d, o-(NC)$_2$C$_6$H$_4$). $^{31}$P{$^1$H} NMR (CD$_3$CN): δ [ppm] = 139.0 (s, [Cp*Fe($\eta^5$-P$_5$)]). $^{19}$F NMR (CD$_3$CN): δ [ppm] = −126.0 (m, SbF$_6$). Positive ion ESI-MS

(CD$_3$CN): 130.2 [o-NC(C$_6$H$_4$)CN]$^{2+}$, 534.9 [{Cp*Fe($\eta^5$-P$_5$)}Ag(CH$_3$CN)$_2$]$^+$, 2178.2 [{Cp*Fe($\eta^5$-P$_5$)}$_4$Ag$_3$(SbF$_6$)$_2$]$^+$. Negative ion ESI-MS (CD$_3$CN): 234.9 [SbF$_6$]$^-$. Elemental analysis: Calculated (%) for [{Cp*Fe($\eta^5$-P$_5$)}$_2$Ag$_3$(o-(NC)$_2$C$_6$H$_4$)$_2$][SbF$_6$]$_3$ (1978.99 g/mol): 21.85 C, 1.94 H, 2.83 N; found: 22.22 C, 2.11 H, 2.70 N. **2)** Yield: 14 mg (14% referred to **A**). $^1$H NMR (CD$_3$CN): δ [ppm] = 1.46 (s, [Cp*Fe($\eta^5$-P$_5$)]), 7.82 (d, o-(NC)$_2$C$_6$H$_4$). $^{31}$P{$^1$H} NMR (CD$_3$CN): δ [ppm] = 137.77 (s, [Cp*Fe($\eta^5$-P$_5$)]). $^{19}$F NMR (CD$_3$CN): δ [ppm] = −126.0 (m, SbF$_6$). Positive ion ESI-MS (CD$_3$CN): 493.9 [{Cp*Fe($\eta^5$-P$_5$)}Ag(CH$_3$CN)]$^+$, 1142.5 [{Cp*Fe($\eta^5$-P$_5$)}$_2$Ag$_2$(SbF$_6$)]$^+$, 1645.4 Ag$_4$(SbF$_6$)$_3$(o-(NC)$_2$C$_6$H$_4$)$_3$(CH$_3$CN)$_3$]$^+$. Negative ion ESI-MS (CH$_3$CN): m/z (%) = 234.9 [SbF$_6$]$^-$. Elemental analysis: Calculated (%) for [{Cp*Fe($\eta^5$-P$_5$)}$_2$Ag$_4$(o-(NC)$_2$C$_6$H$_4$)$_4$][SbF$_6$]$_4$ (2578.86 g/mol): 24.22 C, 1.80 H, 4.35 N; found: 24.60 C, 2.17 H, 4.34 N. **3)** Yield 23 mg (22% referred to **A**). $^1$H NMR (CD$_3$CN): δ [ppm] = 1.46 (s, [Cp*Fe($\eta^5$-P$_5$)]), 7.82 (d, o-(NC)$_2$C$_6$H$_4$). $^{31}$P{$^1$H} NMR (CD$_3$CN): δ [ppm] = 136.44 (s, [Cp*Fe($\eta^5$-P$_5$)]). $^{19}$F NMR (CD$_3$CN): δ [ppm] = −126.0 (m, SbF$_6$). Positive ion ESI-MS (CD$_3$CN): 452.8 [{Cp*Fe($\eta^5$-P$_5$)}Ag]$^+$, 798.7 [{Cp*Fe($\eta^5$-P$_5$)}$_2$Ag]$^+$, 1645.4 Ag$_4$(SbF$_6$)$_3$((NC)$_2$C$_6$H$_4$)$_3$(CH$_3$CN)$_3$]$^+$, 2521.9 [{Cp*Fe($\eta^5$-P$_5$)}$_4$Ag$_4$(SbF$_6$)$_3$]$^+$. Negative ion ESI-MS (CH$_3$CN): m/z (%) = 234.9 [SbF$_6$]$^-$ Elemental analysis: Calculated (%) for [{Cp*Fe($\eta^5$-P$_5$)}$_3$Ag$_4$(o-(NC)$_2$C$_6$H$_4$)$_2$][SbF$_6$]$_4$ (2668.55 g/mol): 20.70 C, 2.00 H, 2.10 N; found: 21.44 C, 2.55 H, 2.08 N.

**Synthesis of 4/5**: A solution of AgSbF$_6$ (28 mg, 0.08 mmol) in CH$_2$Cl$_2$ (20 mL) is carefully layered first with a solvent mixture of CH$_2$Cl$_2$/toluene (5 mL, 2:1) and then with a green solution of [Cp*Fe($\eta^5$-P$_5$)] (14 mg, 0.04 mmol) and m-(NC)$_2$C$_6$H$_4$ (1 mL, 0.4 M in CH$_2$Cl$_2$) in toluene (20 mL). After a few hours, the phase boundary turns yellow, and, after one day, the formation of yellow plates of **4** and brown lath-shaped crystals of **5** at the phase boundary is observed. After complete diffusion, the colorless mother liquor is decanted, the crystals are washed with hexane (3×10 mL) and dried in vacuo. The products were separated manually.

**Analytical data of 4/5**: **4)** Yield: 43 mg (67% referred to **A**). $^1$H NMR (CD$_3$CN): δ [ppm] = 1.46 (s, [Cp*Fe($\eta^5$-P$_5$)]), 7.70 (t, m-(NC)$_2$C$_6$H$_4$), 7.98 (d, m-(NC)$_2$C$_6$H$_4$), 8.00 (s, m-(NC)$_2$C$_6$H$_4$). $^{31}$P{$^1$H} NMR (CD$_3$CN): δ [ppm] = 139.14 (s, [Cp*Fe($\eta^5$-P$_5$)]). $^{19}$F NMR (CD$_3$CN): δ [ppm] = −125.36 (m, SbF$_6$). Positive ion ESI-MS (CH$_3$CN): m/z (%) = 130.2 [m-NC(C$_6$H$_4$)CN]$^{2+}$, 1832.3 [{Cp*Fe($\eta^5$-P$_5$)}$_3$Ag$_3$(SbF$_6$)$_2$]$^+$, 2303.1 [{Cp*Fe($\eta^5$-P$_5$)}$_3$Ag$_4$(SbF$_6$)$_3$(m-(NC)$_2$C$_6$H$_4$)]$^+$. Negative ion ESI-MS (CH$_3$CN): m/z (%) = 234.9 [SbF$_6$]$^-$. Elemental analysis: Calculated (%) for [{Cp*Fe($\eta^5$-P$_5$)}$_2$Ag$_2$(m-(NC)$_2$C$_6$H$_4$)(C$_7$H$_8$)$_{0.5}$(CH$_2$Cl$_2$)$_{0.5}$][SbF$_6$]$_2$ (1595.78 g/mol): 24.09 C, 2.46 H, 1.76 N; found: 23.84 C, 2.59 H, 2.23 N. **5)** Yield: 11 mg (19% referred to **A**). $^1$H NMR (CD$_3$CN): δ [ppm] = 1.45 (s, [Cp*Fe($\eta^5$-P$_5$)]), 7.70 (t, m-(NC)$_2$C$_6$H$_4$), 7.98 (d, m-(NC)$_2$C$_6$H$_4$), 8.11 (s, m-(NC)$_2$C$_6$H$_4$). $^{31}$P{$^1$H} NMR (CD$_3$CN): δ [ppm] = 138.93 (s, [Cp*Fe($\eta^5$-P$_5$)]). $^{19}$F NMR (CD$_3$CN): δ [ppm] = −125.37 (m, SbF$_6$). Positive ion ESI-MS (CH$_3$CN): m/z (%) = 130.2 [m-NC(C$_6$H$_4$)CN]$^{2+}$, 1142.5 [{Cp*Fe($\eta^5$-P$_5$)}$_2$Ag$_2$(SbF$_6$)]$^+$, 1486.3 [{Cp*Fe($\eta^5$-P$_5$)}$_2$Ag$_3$(SbF$_6$)$_2$]$^+$, 1645.4 Ag$_4$(SbF$_6$)$_3$(m-(NC)$_2$C$_6$H$_4$)$_3$(CH$_3$CN)$_3$]$^+$, 2303.1 [{Cp*Fe($\eta^5$-P$_5$)}$_3$Ag$_4$(SbF$_6$)$_3$(m-(NC)$_2$C$_6$H$_4$)]$^+$. Negative ion ESI-MS (CH$_3$CN): m/z (%) = 234.9 [SbF$_6$]$^-$. Elemental analysis: Calculated (%) for [{Cp*Fe($\eta^5$-P$_5$)}Ag$_2$(m-(NC)$_2$C$_6$H$_4$)$_2$(C$_7$H$_8$)(CH$_2$Cl$_2$)][SbF$_6$]$_2$ (1466.51 g/mol): C 27.85, H 2.27, N 3.82; found: C 27.62, H 2.48, N 3.61.

**Synthesis of 6a/b**: In a Schlenk tube, a solution of AgSbF$_6$ (28 mg, 0.04 mmol) in CH$_2$Cl$_2$ (10 mL) is carefully layered first with a solvent mixture of CH$_2$Cl$_2$/toluene (3 mL, 2:1) and then with a green solution of [Cp*Fe($\eta^5$-P$_5$)] (14 mg, 0.04 mmol) and p-(NC)$_2$C$_6$H$_4$ (1 mL, 0.2 M in DCM) in toluene (10 mL). After a few hours, the phase boundary turns yellow, and, after one day, the formation of brown blocks of **6a** at the phase boundary is observed. After complete diffusion, yellow needles of **6b** are found in the bottom of the Schlenk tube. The colorless mother liquor is decanted, the crystals are washed with hexane (3×10 mL) and dried in vacuo. The crystals were sorted manually.

**Chemistry–A European Journal**

Research Article
doi.org/10.1002/chem.202203963

**Chemistry**
**Europe**
European Chemical
Societies Publishing

**Analytical data of 6a/b: 6a)** Yield: 22 mg (45% referred to **A**). $^1$H NMR (CD$_3$CN): $\delta$ [ppm] = 1.46 (s, [Cp*Fe($\eta^5$-P$_5$)]), 7.88 (s, $p$-(NC)$_2$C$_6$H$_4$). $^{31}$P{$^1$H} NMR (CD$_3$CN): $\delta$ [ppm] = 136.78 (s, [Cp*Fe($\eta^5$-P$_5$)]). $^{19}$F NMR (CD$_3$CN): $\delta$ [ppm] = −125.37 (p, SbF$_6$). Positive ion ESI-MS (CH$_3$CN): $m/z$ (%) = 147.9 [Ag(CH$_3$CN)]$^+$, 493.9 [{Cp*Fe($\eta^5$-P$_5$)}Ag(CH$_3$CN)]$^+$, 1486.3 [{Cp*Fe($\eta^5$-P$_5$)}$_2$Ag$_3$(SbF$_6$)$_2$]$^+$, 1645.42 Ag$_4$(SbF$_6$)$_3$($p$-(NC)$_2$C$_6$H$_4$)$_3$(CH$_3$CN)$_3$]$^+$, 1832.3 [{Cp*Fe($\eta^5$-P$_5$)}$_3$Ag$_3$(SbF$_6$)$_2$]$^+$. Negative ion ESI-MS (CH$_3$CN): $m/z$ (%) = 234.9 [SbF$_6$]$^-$. Elemental analysis: Calculated (%) for [{Cp*Fe($\eta^5$-P$_5$)}Ag$_2$($p$-(NC)$_2$C$_6$H$_4$)(CH$_2$Cl$_2$)$_{0.7}$]$_n$[SbF$_6$]$_{2n}$: (1224.16 g/mol): C 18.39, H 1.69, N 2.29; found: C 17.97, H 2.07, N 2.10. **6b)** Yield: 27 mg (29% referred to **A**). $^1$H NMR (CD$_3$CN): $\delta$ [ppm] = 1.46 (s, [Cp*Fe($\eta^5$-P$_5$)]), 7.88 (s, $p$-(NC)$_2$C$_6$H$_4$). $^{31}$P{$^1$H} NMR (CD$_3$CN): $\delta$ [ppm] = 135.45 (s, [Cp*Fe($\eta^5$-P$_5$)]). $^{19}$F NMR (CD$_3$CN): $\delta$ [ppm] = −125.36 (m, SbF$_6$). Positive ion ESI-MS (CH$_3$CN): $m/z$ (%) = 534.9 [{Cp*Fe($\eta^5$-P$_5$)}Ag-(CH$_3$CN)$_2$]$^+$, 798.7 [{Cp*Fe($\eta^5$-P$_5$)}$_2$Ag]$^+$, 1645.42 Ag$_4$(SbF$_6$)$_3$($p$-(NC)$_2$C$_6$H$_4$)$_3$(CH$_3$CN)$_3$]$^+$, 2521.9 [{Cp*Fe($\eta^5$-P$_5$)}$_4$Ag$_4$(SbF$_6$)$_3$]$^+$. Negative ion ESI-MS(CH$_3$CN): $m/z$ (%) = 234.9 [SbF$_6$]$^-$. Elemental analysis: Calculated (%) for [{Cp*Fe($\eta^5$-P$_5$)}Ag$_2$($p$-(NC)$_2$C$_6$H$_4$)]$_n$[SbF$_6$]$_{2n}$ (2322.63 g/mol): 18.62 C, 1.65 H, 2.41 N; found: 19.08 C, 2.21 H, 2.37 N.

**Synthesis of 7**: In a Schlenk tube, a solution of AgSbF$_6$ (14 mg, 0.04 mmol) in CH$_2$Cl$_2$ (8 mL) is carefully layered first with a solvent mixture of CH$_2$Cl$_2$/toluene (2 mL, 2:1) and then with a green solution of [Cp*Fe($\eta^5$-P$_5$)] (14 mg, 0.04 mmol) and $p$-(NC)$_2$C$_6$H$_4$ (51 mg, 0.4 mmol) in toluene (8 mL). After a few hours, the phase boundary turns yellow, and, after one day, the formation of brown prisms **7** at the phase boundary is observed. After complete diffusion, the light green mother liquor is decanted, the crystals are washed with hexane (3×10 mL) and dried *in vacuo*.

**Analytical data of 7**: Yield: 36 mg, (60% referred to **A**). $^1$H NMR (CD$_3$CN): $\delta$ [ppm] = 1.44 (s, [Cp*Fe($\eta^5$-P$_5$)]), 7.87 (s, $p$-(NC)$_2$C$_6$H$_4$)). $^{31}$P{$^1$H} NMR (CD$_3$CN): $\delta$ [ppm] = 141.424 (s, [Cp*Fe($\eta^5$-P$_5$)]). $^{19}$F NMR (CD$_3$CN): $\delta$ [ppm] = −125.38 (m, SbF$_6$). Positive ion ESI-MS (CH$_3$CN): $m/z$ (%) = 130.2 [$p$-NC(C$_6$H$_4$)CN]$^{2+}$, 1832.3 [{Cp*Fe($\eta^5$-P$_5$)}$_3$Ag$_3$(SbF$_6$)$_2$]$^+$. Negative ion ESI-MS (CH$_3$CN): $m/z$ (%) = 234.9 [SbF$_6$]$^-$. Elemental analysis: Calculated (%) for [{Cp*Fe($\eta^5$-P$_5$)}$_2$Ag$_2$($p$-(NC)$_2$C$_6$H$_4$)]$_n$[SbF$_6$]$_{2n}$ (1507.24 g/mol): 22.31 C, 2.27 H, 1.86 N; found: 22.39 C, 2.27 H, 1.75 N.

**Synthesis of 8**: A solution of [Cp″Fe($\eta^5$-P$_5$)] (15.5 mg, 0.04 mmol, 1 equiv.) and $o$-C$_8$H$_4$N$_2$ (1 mL, 0.2 mmol in CH$_2$Cl$_2$, 5 equiv.) in a 1:2 mixture of toluene/hexane (15 mL) is stirred for 3 h at room temperature. Afterwards the reaction mixture is filtered. A solution of AgSbF$_6$ (27.5 mg, 0.08 mmol, 2 equiv.) in CH$_2$Cl$_2$ (15 mL) is first carefully layered by a solvent mixture of CH$_2$Cl$_2$/toluene (4 mL, 2:1) and then by the mixture of [Cp″Fe($\eta^5$-P$_5$)] and $o$-C$_8$H$_4$N$_2$. After one day, the formation of light brown blocks of **8** at the phase boundary is observed. The light brownish mother liquor is decanted, the crystals are washed with hexane (3×15 mL) and CH$_2$Cl$_2$ (4×15 mL) and dried *in vacuo*.

**Analytical data of 8**: Yield: 59 mg (53% referred to **B**). $^1$H NMR (CD$_3$CN): $\delta$ [ppm] = 1.19 (s, C$_5$H$_3^t$Bu$_2$), 4.23 (s, C$_5$H$_3^t$Bu$_2$), 4.28 (s, C$_5$H$_3^t$Bu$_2$), 7.87 (m, C$_8$H$_4$N$_2$)). $^{31}$P NMR (CD$_3$CN): $\delta$ [ppm] = 149.6 (s, [Cp″Fe($\eta^5$-P$_5$)]). $^{19}$F NMR (CD$_3$CN): $\delta$ [ppm] = −122.8 (m, SbF$_6^-$). Positive ion ESI-MS (CH$_3$CN): $m/z$ (%) = 535.89 [{Cp″Fe($\eta^5$-P$_5$)}Ag-(CH$_3$CN)]$^+$, 1026.71 [Ag$_4$($o$-(NC)$_2$C$_6$H$_4$)$_4$(CH$_3$CN)$_2$]$^+$. Negative ion ESI-MS (CH$_3$CN): $m/z$ (%) = 234.89 [SbF$_6$]$^-$. Elemental analysis: Calculated (%) for [{Cp″Fe($\eta^5$-P$_5$)}$_3$Ag$_4$($o$-(NC)$_2$C$_6$H$_4$)]$_n$(SbF$_6$)$_{4n}$ (2794.78 g/mol): 23.64 C, 2.56 H, 2.00 N; found: 23.89 C, 2.81 H, 2.65 N.

**Synthesis of 9**: In a Schlenk tube, a solution of AgSbF$_6$ (27.5 mg, 0.08 mmol, 2 equiv.) in CH$_2$Cl$_2$ (15 mL) is carefully layered first with a solvent mixture of CH$_2$Cl$_2$/toluene (4 mL, 2:1) and then with a green solution of [Cp″Fe($\eta^5$-P$_5$)] (15.5 mg, 0.04 mmol, 1 equiv.) and

$m$-C$_8$H$_4$N$_2$ (1 mL, 0.4 mmol in CH$_2$Cl$_2$, 5 equiv.) in toluene (15 mL). After one day, the formation of green plates of **9** at the phase boundary is observed. The brownish mother liquor is decanted, the crystals are washed with CH$_2$Cl$_2$ (2×5 mL) and pentane (2×5 mL) and dried *in vacuo*.

**Analytical data of 9**: Yield: 32 mg (81% referred to **B**). $^1$H NMR (CD$_3$CN): $\delta$ [ppm] = 1.19 (s, C$_5$H$_3^t$Bu$_2$), 4.24 (s, C$_5$H$_3^t$Bu$_2$), 4.33 (s, C$_5$H$_3^t$Bu$_2$), 5.43 (s, CH$_2$Cl$_2$), 7.27–7.13 (m, C$_8$H$_4$N$_2$). $^{31}$P{$^1$H} NMR (CD$_3$CN): $\delta$ [ppm] = 147.4 (s, [Cp″Fe($\eta^5$-P$_5$)]). $^{19}$F NMR (CD$_3$CN): $\delta$ [ppm] = −78.04 (s, SbF$_6^-$). Positive ion ESI-MS (CH$_3$CN): $m/z$ (%) = 576.92 [{Cp″Fe($\eta^5$-P$_5$)}Ag(CH$_3$CN)$_2$]$^+$, 882.84 [{Cp″Fe($\eta^5$-P$_5$)}$_2$Ag], 1108.99 [Ag$_4$($m$-(NC)$_2$C$_6$H$_4$)$_4$(CH$_3$CN)$_4$]$^+$. Negative ion ESI-MS (CH$_3$CN): $m/z$ (%) = 234.89 [SbF$_6$]$^-$. Elemental analysis: Calculated (%) for [{Cp″Fe($\eta^5$-P$_5$)}$_3$Ag$_3$($m$-(NC)$_2$C$_6$H$_4$)]$_n$[SbF$_6$]$_{3n}$ (1957.79 g/mol): 24.30 C, 2.91 H, 1.21 N; found: 24.41 C, 2.55 H, 0.99 N.

**Synthesis of 10**: A solution of AgSbF$_6$ (27.5 mg, 0.08 mmol, 2 equiv.) in CH$_2$Cl$_2$ (15 mL) is carefully layered first with a solvent mixture of CH$_2$Cl$_2$/toluene (4 mL, 2:1) and then with a green solution of [Cp″Fe($\eta^5$-P$_5$)] (15.5 mg, 0.04 mmol, 1 equiv.) and $p$-C$_8$H$_4$N$_2$ (1 mL, 0.4 mmol in CH$_2$Cl$_2$, 5 equiv.) in toluene (15 mL). After one day, the formation of green plates of **10** at the phase boundary is observed. The crystals are washed with pentane (3×5 mL) and dried *in vacuo*.

**Analytical data of 10**: Yield: 21 mg (60% referred to **B**). $^1$H NMR (CD$_3$CN): $\delta$ [ppm] = 1.19 (s, C$_5$H$_3^t$Bu$_2$), 2.18 (br, H$_2$O), 4.17 (s, C$_5$H$_3^t$Bu$_2$), 4.25 (s, C$_5$H$_3^t$Bu$_2$), 5.44 (s, CH$_2$Cl$_2$), 7.89 (s, C$_8$H$_4$N$_2$). $^{31}$P{$^1$H} NMR (CD$_3$CN): $\delta$ [ppm] = 158.8(s, [Cp″Fe($\eta^5$-P$_5$)]). Positive ion ESI-MS (CH$_3$CN): $m/z$ (%) = 535.89 [{Cp″Fe($\eta^5$-P$_5$)}Ag(CH$_3$CN)]$^+$, 882.84 [{Cp″Fe($\eta^5$-P$_5$)}$_2$Ag]$^+$, 1026.71 [Ag$_4$($p$-(NC)$_2$C$_6$H$_4$)$_4$(CH$_3$CN)$_2$]$^+$. Negative ion ESI-MS (CH$_3$CN): $m/z$ (%) = 234.89 [SbF$_6$]$^-$. Elemental analysis: Calculated (%) for [{Cp″Fe($\eta^5$-P$_5$)}Ag($p$-(NC)$_2$C$_6$H$_4$)$_{0.5}$(CH$_2$Cl$_2$)]$_n$[SbF$_6$]$_n$ (880.64 g/mol): 24.55 C, 2.86 H, 1.59 N; found: 24.17 C, 3.11 H, 0.98 N.

Deposition Numbers 2213602 (**1**), 2213601 (**2**), 2213604 (**3**), 2213600 (**4**), 2213608 (**5**), 2213603 (**6a**), 2213606 (**6b**), 2213605 (**7**), 2213609 (**8**), 2213610 (**9**), 2213607 (**10**) contain the supplementary crystallographic data for this paper. These data are provided free of charge by the joint Cambridge Crystallographic Data Centre and Fachinformationszentrum Karlsruhe Access Structures service.

## Conflict of Interest

The authors declare no conflict of interest.

## Data Availability Statement

The data that support the findings of this study are available in the supplementary material of this article.

[1] J. Mohanty, S. D. Choudhury, N. Barooah, H. Pal, A. C. Bhasikuttan in *Comprehensive supramolecular chemistry II* (Ed.: J. L. Atwood), Elsevier, Amsterdam, **2017**, pp 435–45.

[2] a) H.-J. Schneider, A. K. Yatsimirsky, *Principles and methods in supramolecular chemistry*, Wiley, Chichester, **2000**; b) J. W. Steed, D. R. Turner, K. J. Wallace, *Core concepts in supramolecular chemistry and nanochemistry*, Wiley, Hoboken, NJ, **2007**.

[3] a) K. Tiefenbacher, D. Ajami, J. Rebek, *Angew. Chem. Int. Ed.* **2011**, *50*, 12003; b) L. R. MacGillivray, J. L. Atwood, *Nature* **1997**, *389*, 469; c) W. Wei, W. Li, Z. Li, W. Su, M. Hong, *Chem. Eur. J.* **2013**, *19*, 469; d) D. Niu, Y. Jiang, L. Ji, G. Ouyang, M. Liu, *Angew. Chem. Int. Ed.* **2019**, *58*, 5946.

[4] M. D. Pluth, K. N. Raymond, *Chem. Soc. Rev.* **2007**, *36*, 161.

[5] a) T. Kreickmann, C. Diedrich, T. Pape, H. V. Huynh, S. Grimme, F. E. Hahn, *J. Am. Chem. Soc.* **2006**, *128*, 11808; b) A. V. Virovets, E. Peresypkina, M. Scheer, *Chem. Rev.* **2021**, *121*, 14485.

[6] a) S. Sevim, A. Sorrenti, C. Franco, S. Furukawa, S. Pané, J. deMello, J. Puigmartí-Luis, *Chem. Soc. Rev.* **2018**, *47*, 3788; b) K. Suzuki, M. Kawano, M. Fujita, *Angew. Chem.* **2007**, *46*, 2819; c) V. Patroniak, M. Kubicki, A. Mondry, J. Lisowski, W. Radecka-Paryzek, *Dalton Trans.* **2004**, 3295; d) Y. Chu, A. Saad, P. Yin, J. Wu, O. Oms, A. Dolbecq, P. Mialane, T. Liu, *Chem. Eur. J.* **2016**, *22*, 11756.

[7] M. Fujita, J. Yazaki, K. Ogura, *J. Am. Chem. Soc.* **1990**, *112*, 5645.

[8] a) P. J. Stang, D. H. Cao, S. Saito, A. M. Arif, *J. Am. Chem. Soc.* **1995**, *117*, 6273; b) C. A. Hunter, *Angew. Chem. Int. Ed.* **1995**, *34*, 1079.

[9] a) M. Fujita, Y. J. Kwon, S. Washizu, K. Ogura, *J. Am. Chem. Soc.* **1994**, *116*, 1151; b) M. Fujita, *J. Syn. Org. Chem., Jpn.* **1996**, *54*, 953.

[10] M. Fujita, Y. J. Kwon, O. Sasaki, K. Yamaguchi, K. Ogura, *J. Am. Chem. Soc.* **1995**, *117*, 7287.

[11] a) V. Guillerm, D. Maspoch, *J. Am. Chem. Soc.* **2019**, *141*, 16517; b) S. M. Cohen, Z. Zhang, J. A. Boissonnault, *Inorg. Chem.* **2016**, *55*, 7281; c) H. Kim, C. S. Hong, *CrystEngComm* **2021**, *23*, 1377; d) B. Attenberger, E. V. Peresypkina, M. Scheer, *Inorg. Chem.* **2015**, *54*, 7021; e) M. Elsayed Moussa, B. Attenberger, E. V. Peresypkina, M. Fleischmann, G. Balázs, M. Scheer, *Chem. Commun.* **2016**, *52*, 10004.

[12] H. Brake, E. Peresypkina, A. V. Virovets, W. Kremer, C. Klimas, C. Schwarzmaier, M. Scheer, *Inorg. Chem.* **2021**, *60*, 6027.

[13] a) A. Lennartson, P. Southon, N. F. Sciortino, C. J. Kepert, C. Frandsen, S. Mørup, S. Piligkos, C. J. McKenzie, *Chem. Eur. J.* **2015**, *21*, 16066; b) L. Carlucci, G. Ciani, D. M. Proserpio, S. Rizzato, *CrystEngComm* **2002**, *4*, 413; c) E. Peresypkina, M. Bielmeier, A. Virovets, M. Scheer, *Chem. Sci.* **2020**, *11*, 9067.

[14] a) F. Dielmann, M. Fleischmann, C. Heindl, E. V. Peresypkina, A. V. Virovets, R. M. Gschwind, M. Scheer, *Chem. Eur. J.* **2015**, *21*, 6208; b) E. Peresypkina, C. Heindl, A. Virovets, H. Brake, E. Mädl, M. Scheer, *Chem. Eur. J.* **2018**, *24*, 2503; c) C. Heindl, E. Peresypkina, A. V. Virovets, I. S. Bushmarinov, M. G. Medvedev, B. Krämer, B. Dittrich, M. Scheer, *Angew. Chem. Int. Ed.* **2017**, *56*, 13237; d) C. Heindl, E. Peresypkina, A. V. Virovets, I. S. Bushmarinov, M. G. Medvedev, B. Krämer, B. Dittrich, M. Scheer, *Angew. Chem.* **2017**, *129*, 13420; e) M. Scheer, A. Schindler, R. Merkle, B. P. Johnson, M. Linseis, R. Winter, C. E. Anson, A. V. Virovets, *J. Am. Chem. Soc.* **2007**, *129*, 13386.

[15] E. Peresypkina, K. Grill, B. Hiltl, A. V. Virovets, W. Kremer, J. Hilgert, W. Tremel, M. Scheer, *Angew. Chem.* **2021**, *60*, 12132.

[16] E. Peresypkina, A. Virovets, M. Scheer, *Coord. Chem. Rev.* **2021**, *446*, 213995.

[17] a) M. Detzel, G. Friedrich, O. J. Scherer, G. Wolmershäuser, *Angew. Chem. Int. Ed.* **1995**, *34*, 1321; b) S. Reichl, E. Mädl, F. Riedelberger, M. Piesch, G. Balázs, M. Seidl, M. Scheer, *Nat. Commun.* **2021**, *12*, 5774.

[18] M. Fleischmann, J. S. Jones, F. P. Gabbaï, M. Scheer, *Chem. Sci.* **2015**, *6*, 132.

# RESEARCH ARTICLE

**Coordination polymers**: The combination of the rigid, aromatic dinitrile isomers *ortho/meta/para*-$(NC)_2C_6H_4$, the pentaphosphaferrocenes $[Cp^RFe(\eta^5\text{-}P_5)]$ ($Cp^R$ = Cp*, Cp''; Cp* = $\eta^5\text{-}C_5Me_5$; Cp'' = $\eta^5\text{-}C_5H_3tBu_2\text{-}1,3$) with different steric demands and a silver salt with a non-coordinating anion $SbF_6^-$ gives a unique view into how those building blocks can influence a three-component self-assembly system giving rise to various 1D/2D/3D-coordination polymers.
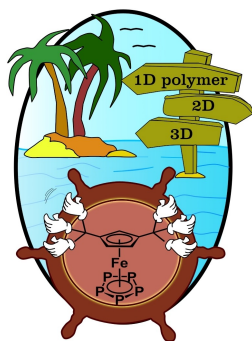


*K. Grill, S. B. Dinauer, Dr. E. Peresypkina, Dr. A. V. Virovets, Prof. Dr. M. Scheer\**

1 – 11

**Across the Dimensions: A Three-Component Self-Assembly of Pentaphosphaferrocene-based Coordination Polymers**